# Upper tropospheric water vapour variability over tropical latitudes observed using radiosonde and satellite measurements

Ghouse Basha[1], M Venkat Ratnam[1,*] and B V Krishna Murthy[2]

[1]*National Atmospheric Research Laboratory (NARL), Department of Space, Government of India, Gadanki, PB No. 123, Tirupati 517 502, India.*
[2]*B1, CEEBROS, 47/20, III Main Road, Gandhi Nagar, Adyar, Chennai 600 020, India.*
*Corresponding author. e-mail: vratnam@narl.gov.in*

The present study deals with using long-term database for upper tropospheric water vapour (UTWV) variability studies over three tropical stations (Gadanki, Singapore and Truk), where different climatic conditions prevail. Over Gadanki (13.5°N, 79.2°E) strong seasonal variation in UTWV is revealed but not over Singapore (1.37°N, 103.98°E) and Truk (7.46°N, 151.85°E) except at 100 hPa. It is examined whether high resolution radiosonde measurements represent well the UTWV by comparing with different satellite based (Atmospheric Infrared Sounder (AIRS), Advanced Microwave Sounding Unit-B (AMSU-B) and Microwave Limb Sounder (MLS)) water vapour measurements. Very good comparison in the nature of variations of UTWV is observed between radiosonde data and satellite data, except over Singapore particularly with AIRS and MLS data, on long-term basis. An attempt is also made to examine the source for UTWV. A close relationship is found between UTWV and deep convection over Gadanki indicating that the source for UTWV is convection particularly during the summer monsoon season.

## 1. Introduction

Water vapour plays a significant role in the Earth's climate. It has direct effect as a greenhouse gas (Linzen 1990) and has indirect effect through its interaction with clouds, aerosols and tropospheric chemistry. Small changes in upper troposphere and lower stratosphere (UTLS) water vapour have great impact on greenhouse effect (Hansen *et al.* 1984). In contrast to warming in the lower troposphere, water vapour leads to cooling in the stratosphere (Forster and Shine 1999). Climate models predict increase in water vapour by 10% for every 1 K increase in temperature at the surface. This sensitivity is greater than that is predicted by Clausius–Clapeyron equation (6% per 1 K at 300 K) (IPCC 2007). Recent study of Solomon *et al.* (2010) using 30 years (1980–2010) of balloon measurements, documents the role of stratospheric water vapour in global climate change. They found that stratospheric water vapour increased from 1980 to 2000 by about 1 part per million by volume (ppmv), while there was a drop of 0.4 ppmv in the later period. They incorporated these changes in the radiative-transfer model and concluded that changes of that magnitude could slow the rate of global surface temperature increase by 25% after the year 2000 and enhance the rate by 30% from 1980 to 2000.

In the tropics, upper tropospheric water vapour measurements are scanty. One of the aims of the present study is to explore for suitable dataset on

**Keywords.** Water vapour; radiosonde; satellite measurements.

upper troposphere water vapour (UTWV) in the tropical region. Therefore, it is examined primarily whether high resolution radiosonde RH measurements can indicate reliable UT humidity (UTH). For this three high resolution radiosonde stations located in the tropical region have been chosen for comparison with Advanced Microwave Sounding Unit-B (AMSU-B) and Atmospheric Infrared Sounder (AIRS) data representing UTH. The radiosonde stations are Gadanki (13.5°N, 79.2°E), which is influenced mainly by the Indian summer monsoon (ISM) where large amount of moisture transport takes place, and Singapore (1.37°N, 103.98°E) and Truk (7.46°N, 151.85°E) in western Pacific where there is convection associated with western pacific warm pool with high Sea Surface Temperatures (SST) occurring throughout the year. Although radiosonde measurements are accurate up to −40°C temperature, in this present study we have utilized high quality radiosonde measurements Väisälä/Meisei over Gadanki and Väisälä over Singapore and Truk (Randel and Wu 2006) which are well calibrated providing data with good vertical resolution. The UTWV from radiosonde is compared with MLS data which represents reliably UTWV. Finally, the relation between UTWV and deep convection in the tropical regions is examined.

## 2. Database

### 2.1 *GPS radiosonde*

High resolution GPS radiosondes are being launched regularly over Gadanki since April 2006. Data of temperature, horizontal wind components and relative humidity are collected with a height resolution of 25–30 m (sampled at 5 s intervals) from Väisälä RS-80 (April 2006 to March 2007) and Meisei RS-01GII sondes (May 2007 to 31 May 2011). Note that there is no difference in the atmospheric parameters retrieved from different receivers used in the present study. Most of these radiosondes were launched around 12 UT (LT = UT + 0530 h). On an average 25 radiosonde observations are available during each month except six observations in December 2006 and no observations during April 2007. The temperature (relative humidity) sensor in Väisälä RS-80 is thermo cap Capacitive bead (HUMICAP thin film capacitor) with a range, accuracy and resolution of −90° to +60°C (0–100%), 0.2°C (5%) and 0.1°C (1%), respectively. In case of Meisei RS-01GII sondes, the temperature (relative humidity) sensors are Thermister (Carbon Humidity sensor) with a range of −90° to +40°C (0–100%), accuracy of 0.2° to 0.5°C (5%) and resolution of 0.1°C (1%). In total, 1067 profiles of temperature (T), pressure (P), relative humidity (RH), and horizontal wind are obtained in different seasons. Data has been collected from January 2000 to May 2011 from the other two radiosonde stations, Singapore and Truk. This data has been taken from University of Wyoming website (http://weather.uwyo.edu/upperair/sounding.html). At these two stations, radiosondes were released two times per day (00 UT and 12 UT). However, only 12 UT data has been taken to maintain uniformity with Gadanki data. All the profiles were gridded to 100 m vertical resolution so as to remove outliers from the random motion of balloon (Tsuda *et al.* 2006).

### 2.2 *Atmospheric Infrared Sounder (AIRS) data*

AIRS is onboard NASA's Earth observing system satellite Aqua (EOS-Aqua), which is in a sun-synchronous polar orbit with equatorial crossing at ∼1330 and ∼0130 LT. The AIRS is accompanied by two microwave sounding radiometers, namely Advanced Microwave Sounding Unit-A (AMSU-A) and Humidity Sounder for Brazil (HSB). It has a field-of-view of 1.1° and provides a nominal spatial resolution of ∼13.5 km for IR channels and ∼2.3 km for visible/near-IR channels. The AIRS instrument provides several parameters including vertical profiles of atmospheric water vapour. In this study, the daily level-3 products of Aqua/AIRS (version 5) are used, and they are acquired from the NASA's GES-DISC Interactive Online Visualization and Analysis Infrastructure (Giovanni) (http://gdata1.sci.gsfc.nasa.gov/daac-bin) with 12 pressure levels starting from 1000–100 hPa and horizontal resolutions are 1 × 1° latitude and longitude. Water vapour profiles are with an accuracy of 20% per 2 km thick layer in the lower troposphere and 20–60% in the upper troposphere (Divakarla *et al.* 2006).

### 2.3 *Advanced Microwave Sounding Unit-B (AMSU-B) data*

AMSU-B is a cross-track scanning microwave sensor with channels at 89.0, 150.0, 183.31 ± 1.00, 183.31 ± 3.00, and 183.31 ± 7.00 GHz (Saunders *et al.* 1995). These channels are called channels 16–20 of the overall AMSU; channels 1–15 belong to AMSU-A. The instrument has a swath width of approximately 2300 km, which is sampled at 90 scan positions. The satellite viewing angle for the innermost scan positions is 0.55° from nadir; for the outermost scan positions, it is 48.95° from nadir. This corresponds to incidence angles of 0.62° and 58.5° from nadir, respectively.

Table 1. *Starting and ending dates of different dataset available from different techniques for UTH.*

| Instrument | Starting date | Ending date |
|---|---|---|
| Radiosonde | | |
| Gadanki | 2006–04 | 2011–05 |
| Singapore | 2000–01 | 2011–05 |
| Truk | 2000–01 | 2011–05 |
| AIRS | 2002–09 | 2011–05 |
| MLS | 2005–01 | 2011–05 |
| NOAA-15 | 2000–01 | 2009–04 |
| NOAA-16 | 2000–09 | 2009–04 |
| NOAA-17 | 2002–06 | 2009–04 |
| NOAA-18 | 2005–05 | 2008–12 |
| METOPA | 2006–10 | 2008–12 |

The footprint size is $20\times16$ km$^2$ for the innermost scan positions but increases to $64\times52$ km$^2$ for the outermost positions. The current version (uth-data-v2d.tar.bz2) of AMSU-B has been taken from http://www.sat.ltu.se/projects/uth-clim/ which has a spatial resolution of 2.5° × 2.5° latitude and longitude grid. In this study, AMSU-B data available from NOAA-15, 16, 17, 18, and METOPA are used. Data availability from different satellites is shown in table 1.

### 2.4 *Microwave Limb Sounder (MLS)*

Earth Observing System (EOS) Microwave Limb Sounder (MLS), NASA Aura satellite launched on 15 July 2004 uses the microwave limb sounding technique (Waters *et al.* 2006) to provide information on water vapour in UT, stratosphere and mesosphere. MLS version 2.2 (V2.2) Level 2 water vapour dataset whose validations are described by Read *et al.* (2007) is used in the present study for the period from 1 January 2005 to 31 May 2011. MLS measures ∼3500 vertical profiles per day along a sun-synchronous suborbital track having equatorial crossings at 0140 PM and 0140 AM local solar times. The Level 2 data are produced for 47 pressure surfaces from 1000 to 1E-4 hPa. The vertical resolution of MLS water vapour data is ∼2.5 km around 316–215 hPa, ∼3 km around 100–0.1 hPa.

We have averaged daily radiosonde data in each month to get monthly averaged relative humidity for all the months and for all the different datasets. For UTH comparison NOAA, AIRS and MLS data has been chosen only whenever the radiosonde data is available. The radiosonde data has been averaged over different altitudes for different sensors, i.e., for NOAA, AIRS (500–200 hPa) and for MLS (316–215 hPa). Note that UTH is the integrated product from AMSU-B satellites whereas the UTWV is vertical profile of water vapour from MLS satellite.

### 2.5 *Satellite observations of equivalent blackbody brightness temperature (TBB)*

Hourly cloud top equivalent blackbody temperature, called Brightness Temperature (BT) from MTSAT-1R (Multi-functional Transport SATellite) data provided by the Japan Meteorological Agency (JMA) through Kochi University, Japan is also used. Data were recorded in longitude/latitude grids of 0.05° between 11°–15°N latitude and 77°–81°E longitude covering the location of Gadanki. The TBB data, averaged from the pixel data, are used to examine the characteristics of meso-scale cloud systems. This data has been used as a proxy for tropical deep convection from January 2005 to May 2011. For Singapore and Truk, the Outgoing Long wave Radiation (OLR) data obtained from the National Oceanic and Atmospheric Administration with 2.5° × 2.5° resolution has been used. Values of TBB/OLR less than 240 K or W/m$^2$ are generally considered to represent deep convection.

## 3. Methodology for retrieval of UTH from AMSU-B

Attempt has been made by Soden and Bretherton (1993) to relate the IR radiance to UTH. They reported a log-linear relation between the brightness temperature of 6.7 $\mu$m band from GOES-7 and Jacobian weighted RH in UT (∼500–200 hPa) with an accuracy of ±1 K or ±10% RH. Buehler and John (2005) adopted this for microwave measurements, i.e., AMSU-B data for retrieving Jacobian weighted UTH. A global UTH dataset is derived from radiance of AMSU instruments onboard NOAA satellites which is described by Buehler *et al.* (2008). UTH from AMSU-B is retrieved through log-linear relationship shown below from 181.31 + 1.00 GHz radiance (Buehler and John 2005).

$$\ln(\mathrm{UTH}) = a + b \cdot T_b,$$

where $T_b$ is the radiance brightness temperature and $a$ and $b$ are linear fit coefficients.

UTH from AMSU-B has been compared with radiosonde data over different radiosonde stations across the globe (e.g., Buehler and John 2005; John and Buehler 2005; Buehler *et al.* 2008); but in tropical region, especially over the Indian region, the comparison between radiosonde and AMSU-B has not been done due to lack of high resolution radiosonde data.

## 4. Results and discussion

### 4.1 *Comparison of UTH (∼500–200 hPa) between radiosonde and satellite data*

The RH averaged between the pressure levels 500 and 200 hPa is used to represent UTH. The UTH thus obtained from radiosonde data over Gadanki, Singapore and Truk is compared with the corresponding UTH from AIRS, AMSU-B data and is shown in figure 1. The MLS data has been averaged from 316 to 215 hPa. The starting and ending times of different datasets are shown in table 1. The monthly mean TBB data over Gadanki and OLR data over Singapore and Truk have been taken at the nearest grid of the radiosonde station. AMSU-B and radiosonde show good comparison both in the nature of variations and in magnitude in all the stations. It is evident that UTH over Gadanki (figure 1a) and Truk (figure 1c) shows clear seasonal variation with maximum in summer and minimum in winter. Over Singapore (figure 1b), no such seasonal variation is evident. AIRS UTH shows slightly higher values than radiosonde values over Gadanki and Singapore but matches well over Truk. A strong negative correlation is noticed between TBB and UTH over Gadanki and between OLR and UTH over Truk. However, the correlation is not so strong over Singapore. Thus, increase in convective activity (represented by low values of TBB/OLR) is, in general, associated with increase in UTH. This evidently indicates that deep convection leads to moistening of the UT. From the above it appears that high resolution radiosonde data represents UTH on long-term basis. This is further supported by correlation analysis described in the following.

Figure 2 shows scatter plot of UTH from radiosonde and the three different satellites. A very good correlation is noticed between radiosonde and satellite UTH data over Gadanki and Truk. However, the correlation is comparatively low over Singapore. In fact the correlation of radiosonde with MLS data is very low at Singapore. It is evident that UTH from radiosonde compares well with the satellite data suggesting that it is reliable on long term basis. It is to be noted that Moradi *et al.* (2010) also reported high correlation between AMSU-B and radiosonde over three western pacific stations. Singapore which lies in the warm pool region appears to be an exception. Figure 3 shows

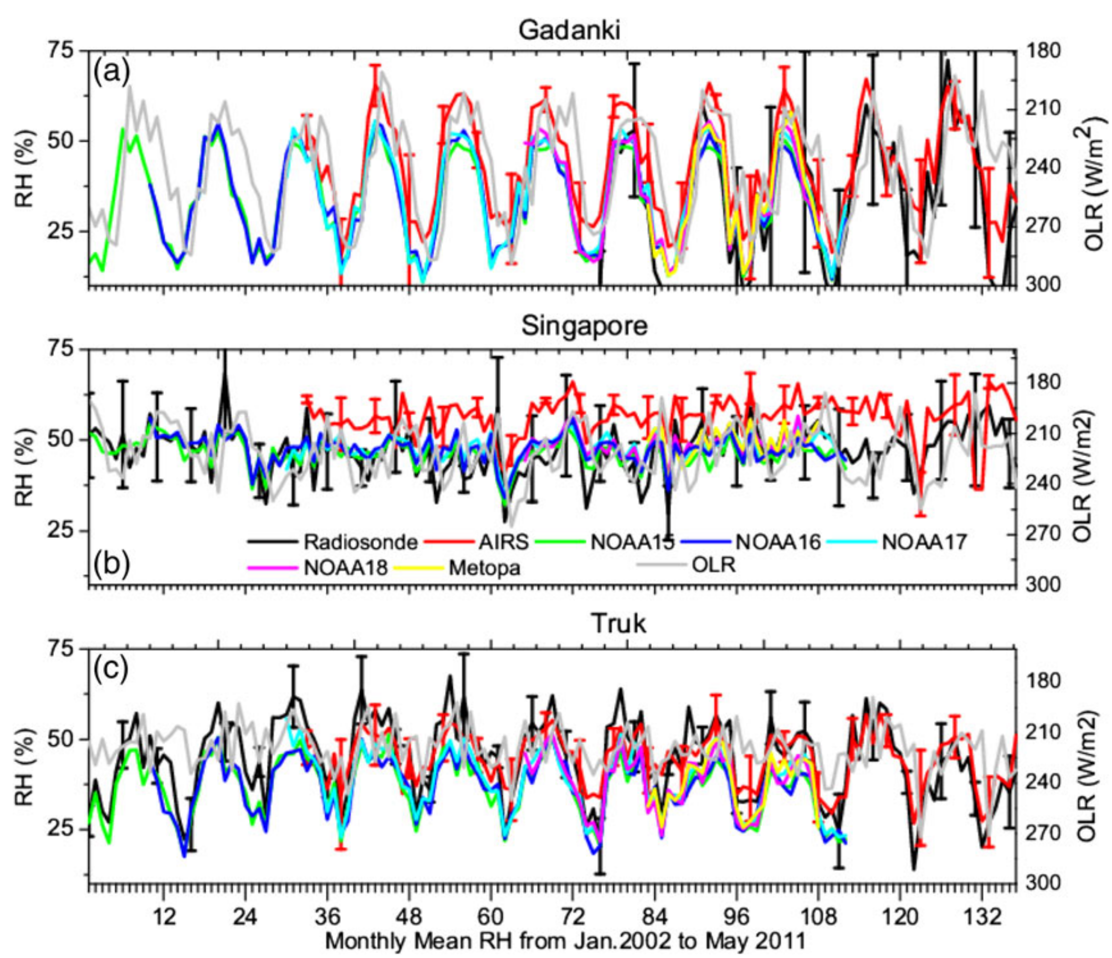


Figure 1. Monthly mean Upper Tropospheric Humidity (UTH) over (**a**) Gadanki, (**b**) Singapore, and (**c**) Truk observed by GPS radiosonde (black), NOAA15 (green), NOAA16 (blue), NOAA17 (cyan), NOAA18 (magenta), METOPA (yellow), and AIRS (red). Monthly mean TBB/OLR is shown in grey color. Relative humidity from GPS radiosonde and AIRS are averaged between 500 and 200 hPa. Vertical bars show the standard deviation.

scatter plot of OLR and UTH from radiosonde, AIRS, MLS and NOAA over Gadanki (3a–d), Singapore (3e–h) and Truk (3i–l). High correlation is found over Gadanki and Truk but it is low over Singapore station.

### 4.2 *UTWV variations*

In the previous section it is shown that high resolution radiosonde data (averaged between 500 and 200 hPa) represents well the UTH. Since the main aim is to examine whether radiosonde measurements represent UTWV, we compared the radiosonde water vapour profiles and MLS profiles. It is well known that, in general, radiosonde RH data is accurate up to −40°C, i.e., up to mid-troposphere. But in the UT, it is questionable. We have taken MLS (at 215 and 100 hPa) data which is very reliable in the UT (but not in the lower troposphere) and AIRS (at 215 hPa) data which provides accurate water vapour measurements for comparison with radiosonde data. Figure 4 shows the monthly mean variation of water vapour at two different pressure levels over Gadanki, i.e., 100 (figure 4a) and 215 hPa (figure 4b) along with OLR (figure 4c). In figure 4(a), temperature at 100 hPa is also shown. The water vapour from radiosonde and MLS at two pressure levels and OLR show clear seasonal variation with maximum during the Indian summer monsoon (ISM) (June, July and August (JJA)) reaching minimum during winter (December, January and February (DJF)). At 100 hPa level, the water vapour from MLS is lower than that from radiosonde. The temperature at 100 hPa shows, variations similar to that of water vapour which means that lower temperature is associated with lower water vapour and *vice versa.* Note that at 100 hPa, the water vapour and temperature prior to April 2007 were obtained from Väisälä RS-80 sondes and these appear to differ substantially from the variation of MLS. But the

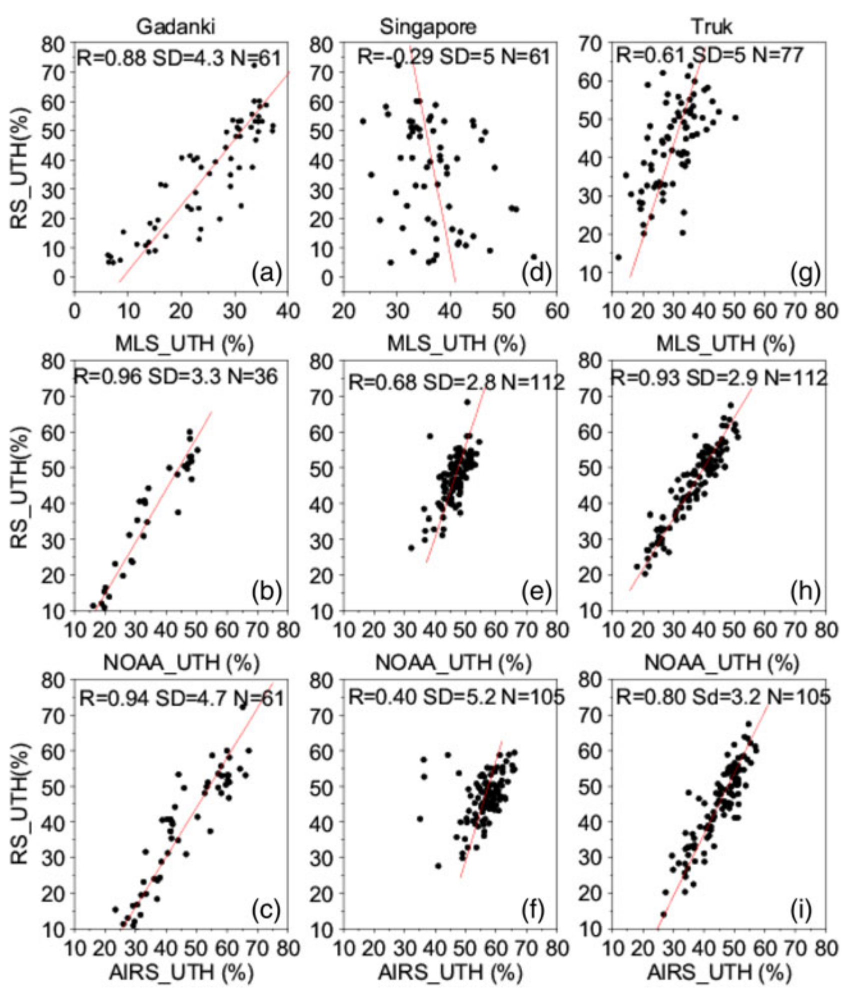


Figure 2. The comparisons of monthly mean radiosonde UTH with MLS, NOAA and AIRS over Gadanki (**a–c**), Singapore (**d–f**) and Truk (**g–i**).

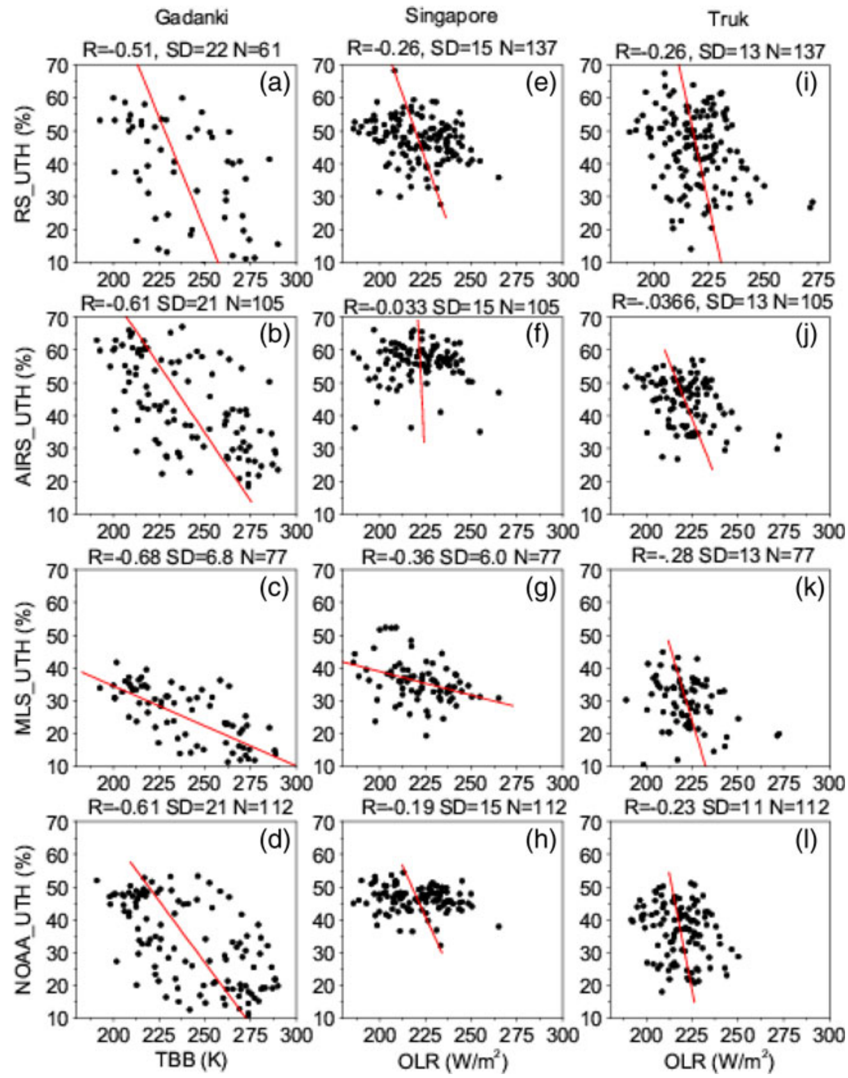


Figure 3. Comparison of TBB/OLR with UTH from radiosonde, AIRS, MLS and NOAA over Gadanki (**a**–**d**), Singapore (**e**–**h**) and Truk (**i**–**l**).

variations in water vapour and temperature from April 2007 onwards from Meisei RS-01GII seem to follow well with MLS water vapour, except in some months after January 2010. Figure 4(b) shows the UTWV variation at 215 hPa between radiosonde, AIRS and MLS. It is evident that radiosonde and AIRS show good comparison than MLS. This result strongly supports that high resolution radiosonde provides accurate water vapour information even at 215 hPa. Similar variation can be noticed in OLR, i.e., deep convection represents higher water vapour UT. Thus, deep convection can induce water vapour in UT.

Figure 5 shows the monthly mean variation of water vapour, temperature and OLR over Truk. The water vapour and temperature at 100 hPa show clear seasonal variation with maximum during NH summer and minimum during winter. However, the seasonal variation is not clear at the lower level. AIRS and radiosonde UTWV show good comparison at 215 hPa with clear seasonal variation as noticed over Gadanki region. Figure 6 shows the monthly mean variations of UTWV, temperature and OLR over Singapore station. Similar to Truk, clear seasonal variation is observed only at 100 hPa. At 215 hPa, AIRS shows high UTWV than radiosonde and MLS but no seasonal variation is observed. This behaviour is in contrast to that over Gadanki where water vapour at these levels showed clear seasonal variations. Note that these values agree well with the one that is reported using frost hygrometer over equatorial region (Vömel *et al.* 2002). At 100 hPa similar features are noticed as that over Gadanki but not at other pressure levels.

It is noticed that OLR values are very low both at Singapore and Truk throughout the year in contrast to the behaviour over Gadanki which

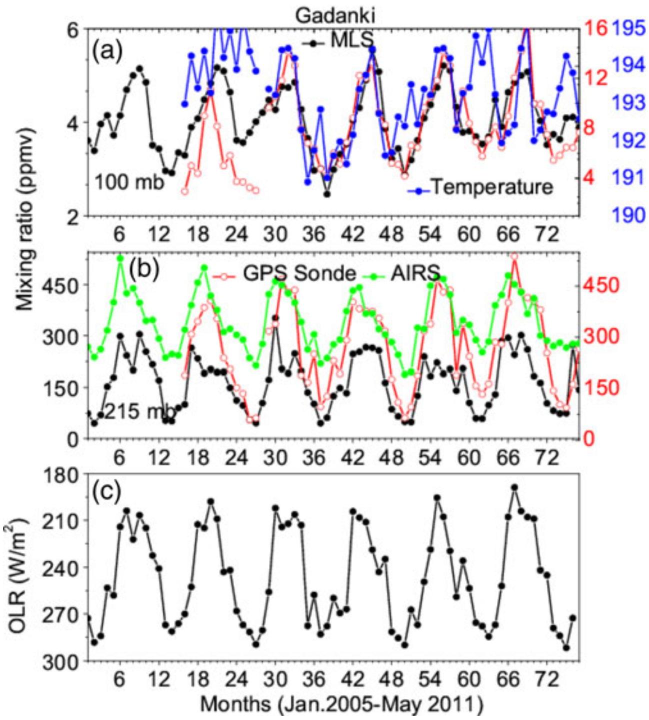


Figure 4. Monthly mean water vapour mixing ratio (ppmv) observed by Aura MLS satellite (red), GPS radiosonde water vapour (black) and temperature (K) (blue), at (**a**) 100 hPa and (**b**) 215 hPa pressure levels over Gadanki. (**c**) Monthly mean TBB over Gadanki.

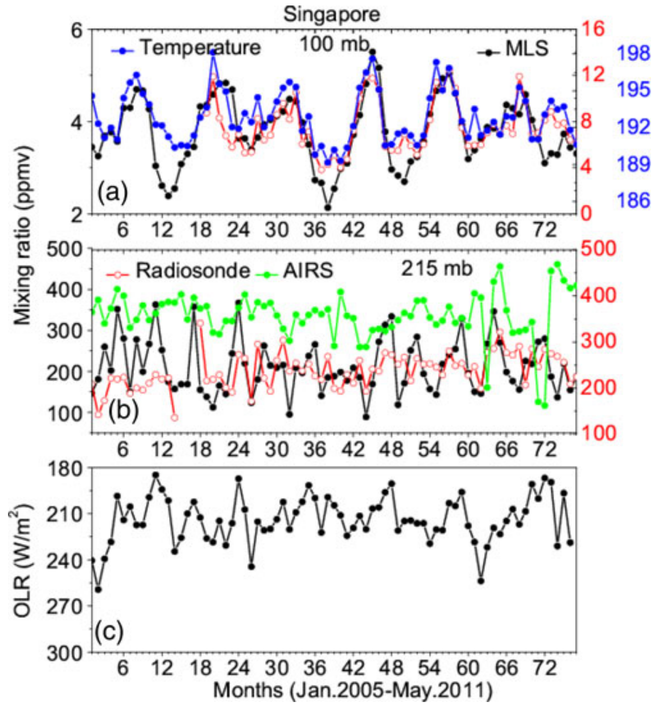


Figure 6. Same as figure 4, but over Singapore.

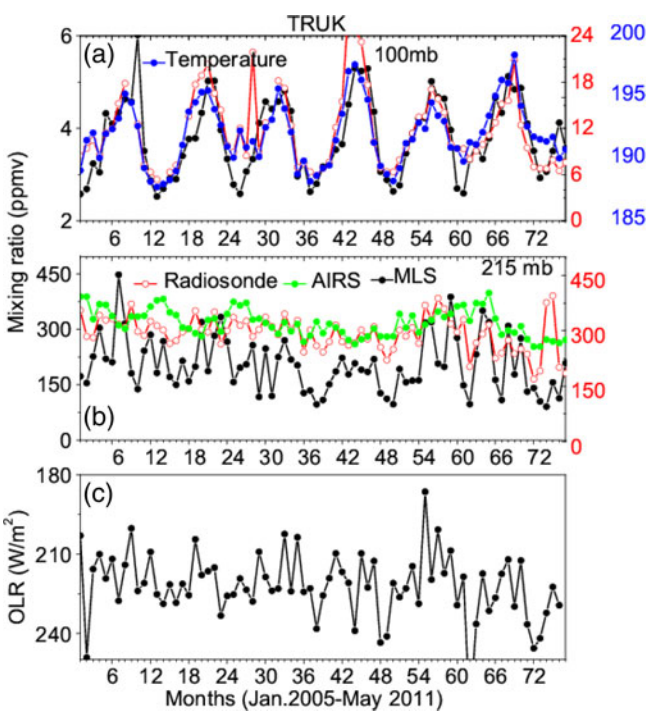


Figure 5. Same as figure 4, but over Truk.

shows low TBB values only during summer. Deep convection throughout the year over Singapore and Truk accounts for the lack of seasonal variation in water vapour at 215 hPa. On the other hand, at 100 hPa level clear seasonal variation is noticed. At 100 hPa, temperature modulate water vapour accounting for lower water vapour in winter and higher in summer. This is manifested as seasonal variation in water vapour. A close look at 100 hPa reveals that the temperature and water vapour variations do not show one-to-one correlations though the variations are similar. In this context it is worth to refer Fueglistaler *et al.* (2009) where they showed good relation between the spatial and temporal patterns of water vapour concentrations and deep convection up to 150 hPa. In the topical tropopause layer, minima in water vapour concentrations are reported in the regions of low temperature anomalies (their figure 5) similar to that observed in our case.

Note that the temperature at 100 hPa Singapore is lower than that at Gadanki and Truk. Water vapour from radiosonde over the three stations is higher in magnitude compared to MLS. From figure 3, the presence of water vapour during the ISM in the UT and also the strong anticorrelation between TBB and UTWV reveal that during deep convection most of the water vapour is transported to higher altitudes. In order to further study the water vapour in UT, the cloud top temperature obtained from TBB is compared with the radiosonde temperature over Gadanki. Although this analysis is not quantitative, here we made an effort to verify whether deep convection will induce water vapour in UT. The equivalent

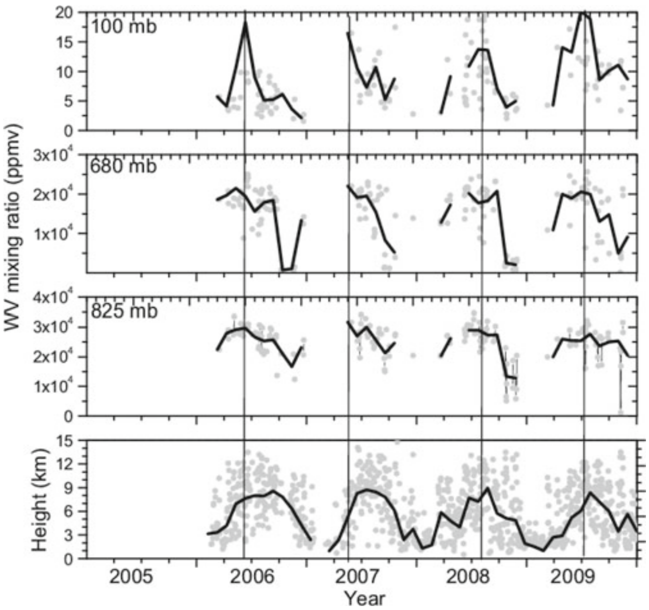


Figure 7. Daily (dots) and monthly mean (line) water vapour mixing ratio over Gadanki from GPS radiosonde at (**a**) 100 hPa, (**b**) 685 hPa and (**c**) 825 hPa pressure levels. (**d**) Variation of daily and monthly mean cloud top altitudes is >10 km.

height represents the cloud top height and is shown in figure 7(d). This analysis will help to locate up to what vertical extent convection is active. Figure 7(a–c) represents time series of daily and monthly mean radiosonde Water Vapour Mixing Ratio (WVMR) at 100, 680, and 825 hPa pressure levels where cloud top height greater than 10 km is noticed. From figure 7(d), it is seen that during NH summer convection reaches an altitude of ≥12 km. OLR shows a clear annual cycle with NH summer having larger extent than NH winter, with clear seasonal variation from NH summer to NH winter. Much of the annual variability is found during NH summer and suppressed during NH winter. The cloud top is broad at 825 hPa and becomes narrower at the lower pressure levels. The presence of water vapour during ISM in UT (figure 7) and strong anti-correlation between TBB and UTWV reveal that during deep convection water vapour is transported to higher altitudes.

## 5. Summary and conclusions

In this study, we made an attempt to verify long-term variation of UTWV using radiosonde data over Gadanki, Truk and Singapore and AMSU-B data. MLS (Janurary 2005–May 2011), AIRS satellite data are also analyzed and compared with the *in-situ* radiosonde water vapour data. Gadanki lies in the ISM region whereas Singapore lies over the warm pool region and Truk in the Pacific region. Very good comparison between radiosonde and AMSU-B UTH is noticed with clear seasonal variation suggesting that high resolution radiosonde measurements represent UTH well. AIRS UTH is higher than radiosonde and AMSU-B. All the datasets show similar behaviour over all the stations with different magnitudes. The main conclusions are summarized below:

1. The seasonal variation of UTH is similar to that of TBB over Gadanki. This is not clear over Singapore and Truk (with OLR) due to presence of convection throughout the year in contrast to Gadanki.
2. Very good comparison is observed between radiosonde and AIRS data at 215 hPa over Gadanki, Truk, but over Singapore AIRS shows higher than radiosonde.
3. The UTWV variation from radiosonde and MLS also shows good comparison in the nature of variations, i.e., water vapour being higher in NH summer and minimum in NH winter over Gadanki at 100 and 215 hPa levels, but differ slightly in magnitude (radiosonde shows more water vapour, 2 times higher than MLS at 100 hPa at all the stations).
4. Over Singapore and Truk, clear seasonal variation in UTWV is revealed only at 100 hPa but not at the lower level (215 hPa) and this is attributed to modulation of seasonal variation of temperature at 100 hPa level.

We noticed strong relation between 100 hPa temperatures, TBB, and UTWV similar to that reported by Read *et al.* (2004). Higher UTWV is associated with deep convection and minimum tropopause temperatures. Therefore, it seems unlikely that deep convection over land could be drying the tropical tropopause layer. It appears that convection overshooting occurs only during deep convection. In general, it is believed that radiosonde RH is accurate up to −40°C and above that RH measurement includes large errors. However, from the present study radiosonde and MLS WVMR showed clear seasonal variation though they differ in magnitudes. Thus, the main conclusion drawn from the present study is that we can use radiosonde for studying the UTH on long term basis. In future it is planned to launch the CFH radiosonde with which it is possible to measure the vertical profile of WVMR up to stratospheric heights.

## Acknowledgements

The authors wish to thank the various data sources for providing satellite data through their FTP sites.

## References

Buehler S A and John V O 2005 A simple method to relate microwave radiances to upper tropospheric humidity; *J. Geophys. Res.* **110** D02110, doi: 10.1029/2004JD005111.

Buehler S A, Kuvatov M, John V O, Milz M, Soden B J, Jackson D L and Notholt J 2008 An upper tropospheric humidity dataset from operational satellite microwave data; *J. Geophys. Res.* **113** D14110, doi: 10.1029/2007JD009314.

Divakarla M G, Barnet C D, Goldberg M D, McMillin L M, Maddy E, Wolf W, Zhou L and Liu X 2006 Validation of atmospheric infrared sounder temperature and water vapour retrievals with matched radiosonde measurements and forecasts; *J. Geophys. Res.* **111** D09S15, doi: 10.1029/2005JD006116.

Forster E F and Shine K P 1999 Stratospheric water vapour changes as a possible contributor to observed stratospheric cooling; *Geophys. Res. Lett.* **2621** 3309–3312, doi: 10.1029/1999GL010487.

Fueglistaler S, Dessler A E, Dunkerton T J, Folkins I, Fu Q and Mote P W 2009 Tropical tropopause layer; *Rev. Geophys.* **47** RG1004, doi: 10.1029/2008RG000267.

Hansen J, Lacis A, Rind D, Russell G, Stone P, Fung I, Ruedy R and Lerner J 1984 Climate sensitivity: Analysis of feedback mechanisms; In: *Climate Processes and Climate Sensitivity* (eds) Hansen J E and Takahashi T, AGU Geophysical Monograph 29, Maurice Ewing, Vol. 5. American Geophysical Union, pp. 130–163.

Intergovernmental Panel on Climate Change IPCC 2007 Climate Change 2007; The Physical Science Basis. Contribution of Working Group I to the Fourth Assessment Report of the Intergovernmental Panel on Climate Change (eds) S Solomon *et al.*, Cambridge University Press, Cambridge, UK.

John V O and Buehler S A 2005 Comparison of microwave satellite humidity data and radiosonde profiles: A survey of European stations; *Atmos. Chem. Phys.* **5** 1843–1853, SRef-ID: 1680-7324/acp/2005-5-1843.

Linzen R S 1990 Some coolness concerning global warming; *Bull. Am. Meteor. Soc.* **71** 288–299.

Moradi I, Buehler S A, John V O and Eliasson S 2010 Comparing upper tropospheric humidity data from microwave satellite instruments and tropical, radiosonde; *J. Geophys. Res.* **115** D24310.

Randel W J and Wu F 2006 Biases in stratospheric and tropospheric temperature trends derived from historical radiosonde data; *J. Climate* **19** 2094–2104.

Read W G, Wu D L, Waters J W and Pumphrey H C 2004 Dehydration in the tropical tropopause layer: Implications from the UARS Microwave Limb Sounder; *J. Geophys. Res.* **109** D06110, doi: 10.1029/2003JD004056.

Read W G *et al.* 2007 Aura Microwave Limb Sounder upper tropospheric and lower stratospheric $H_2O$ and relative humidity with respect to ice validation; *J. Geophys. Res.* **112** D24, doi: 10.1029/2007JD008752.

Saunders R W, Hewison T J, Stringer S J and Atkinson N C 1995 The radiometric characterization of AMSU-B; *IEEE Trans. Microwave Theory Tech.* **434** 760–771.

Soden B J and Bretherton F P 1993 Upper-tropospheric relative-humidity from the GOES 6.7 mm channel: Method and climatology for July 1987; *J. Geophys. Res.* **98** 16,669–16,688.

Solomon S, Rosenlof K, Portmann R, Daniel J, Davis S, Sanford T and Plattner G-K 2010 Contributions of stratospheric water vapour to decadal changes in the rate of global warming; *Science* **327** 1219–1223, doi: 10.1126/science.1182488.

Tsuda T, Venkat Ratnam M, Kozu T and Mori S 2006 Characteristics of 10-day Kelvin wave observed with radiosondes and CHAMP/GPS occultation during CPEA campaign April–May 2004; *J. Meteorol. Soc. Japan* **84A** 277–293.

Vömel H *et al.* 2002 Balloon-borne observations of water vapour and ozone in the tropical upper troposphere and lower stratosphere; *J. Geophys. Res.* **107** 4210, doi: 10.1029/2001JD000707.

Waters J W *et al.* 2006 The Earth Observing System Microwave Limb Sounder EOS MLS on the Aura satellite; *IEEE Trans. Geosci. Remote Sens.* **445** 1075–1092, doi: 10.1109/TGRS.2006.87377.

*MS received 6 December 2012; revised 24 May 2013; accepted 27 May 2013*